Meta-Analytic Connectivity Modeling Reveals Differential Functional Connectivity of the Medial and Lateral Orbitofrontal Cortex

David H. Zald[1,2], Maureen McHugo[3], Kimberly L. Ray[4], David C. Glahn[5], Simon B. Eickhoff[6,7] and Angela R. Laird[4,8]

[1]Department of Psychology, [2]Department of Psychiatry, [3]Vanderbilt Brain Institute, Vanderbilt University, Nashville, TN, USA [4]Research Imaging Institute, University of Texas Health Science Center at San Antonio, San Antonio, TX, USA [5]Department of Psychiatry, Institute of Living, Yale University, Olin Neuropsychiatric Research Center, Hartford, CT, USA [6]Institute of Neuroscience and Medicine (INM-1), Juelich Research Centre, Julich, Germany [7]Institute for Clinical Neuroscience and Medical Psychology, Heinrich-Heine University, Düsseldorf, Germany and [8]Department of Physics, Florida International University, Miami, FL, USA

Address correspondence to D.H. Zald, PMB 407817, 111, 21st Avenue South, NSV, TN 37240-7817, USA. Email: david.zald@vanderbilt.edu

The orbitofrontal cortex (OFC) is implicated in a broad range of behaviors and neuropsychiatric disorders. Anatomical tracing studies in nonhuman primates reveal differences in connectivity across subregions of the OFC, but data on the connectivity of the human OFC remain limited. We applied meta-analytic connectivity modeling in order to examine which brain regions are most frequently coactivated with the medial and lateral portions of the OFC in published functional neuroimaging studies. The analysis revealed a clear divergence in the pattern of connectivity for the medial OFC (mOFC) and lateral OFC (lOFC) regions. The lOFC showed coactivations with a network of prefrontal regions and areas involved in cognitive functions including language and memory. In contrast, the mOFC showed connectivity with default mode, autonomic, and limbic regions. Convergent patterns of coactivations were observed in the amygdala, hippocampus, striatum, and thalamus. A small number of regions showed connectivity specific to the anterior or posterior sectors of the OFC. Task domains involving memory, semantic processing, face processing, and reward were additionally analyzed in order to identify the different patterns of OFC functional connectivity associated with specific cognitive and affective processes. These data provide a framework for understanding the human OFC's position within widespread functional networks.

Keywords: fMRI, network, orbital frontal, ventromedial prefrontal, ventrolateral prefrontal

Introduction

The orbitofrontal cortex (OFC), occupying the ventral surface of the frontal lobe, has been implicated in a broad range of psychological functions and is associated with the pathophysiology of several psychiatric and neurological disorders (Zald and Rauch 2006). Although many researchers refer to the entire region as the OFC or "orbital frontal cortex," substantial evidence indicates that further parcellation is both possible and beneficial (Walker 1940; Barbas and Pandya 1989; Carmichael and Price 1994; Hof et al. 1995; Zald and Kim 1996a, 1996b; Petrides and Mackey 2006; Uylings et al. 2010). In particular, histological staining and anatomical connectivity studies in nonhuman primates have revealed that the OFC is not homogenous, but consists of several cytoarchitectural subregions that possess distinct connections with cortical and subcortical structures (Cavada et al. 2000; Barbas 2007; Price 2007). To date, these anatomical tracing studies in nonhuman primates (supported by diffusion-weighted tractography imaging in humans: Croxson et al. 2005; Malykhin et al. 2011)

have provided the primary foundation for characterizing the features of OFC circuits. However, data from human neuroimaging studies are increasingly able to complement these structural perspectives by detailing the functional connectivity (i.e., patterns of coactivations) of the human OFC. For instance, using resting-state functional magnetic resonance imaging (fMRI), Kahnt et al. (2012) demonstrated that the OFC can be parcellated into several distinct regions. Yet, to date, there has been no systematic attempt to utilize existent human neuroimaging literature to provide insights into the functional delineation of the OFC.

Recently, Robinson et al. (2010) introduced meta-analytic connectivity modeling (MACM) as a technique for assessing the task-based functional connectivity. MACM investigates all activation foci of experiments that report activation within a given seed region and identifies those brain regions where the activation foci accumulate using statistical inference about the likelihood of coactivation with a given seed (cf. Eickhoff and Grefkes 2011). These brain regions can be interpreted as coactivated with the seed region at an above-chance frequency and hence functionally connected. The MACM approach has been used to investigate the functional connectivity of a number of brain regions, including the amygdala (Robinson et al. 2010), somatosensory cortex (Eickhoff et al. 2010), and regions of the default mode network (Laird, Eickhoff, Li 2009).

To provide an initial characterization of the task-based functional connectivity of the OFC, we first divided the OFC into medial and lateral divisions. The medial/lateral distinction arose originally from lesion studies in nonhuman primates, which frequently observed differential behavioral and cognitive effects of medial OFC (mOFC) versus lateral OFC (lOFC) lesions (Zald and Kim 1996b). Evidence for a similar functional division also emerges in human neuroimaging studies (Kringelbach and Rolls 2004). Tracing studies in nonhuman primates further emphasize dissociable patterns of connections between medial and lateral aspects of the OFC (Carmichael and Price 1995a, 1995b). For instance, the lOFC receives inputs from later stages within the visual processing stream (Barbas 1988; Carmichael and Price 1995b), whereas medial regions show strong connections with autonomic centers (Carmichael and Price 1995a).

We further performed contrast analyses of the anterior versus posterior divisions of the mOFC and lOFC regions. Neuroanatomical studies in nonhuman primates indicate that the cytoarchitecture changes from agranular and dysgranular

cortex in the posterior OFC to progressively more densely granular isocortex in the anterior OFC (Barbas and Pandya 1989; Morecraft et al. 1992). This cytoarchitectural trend is paralleled by the structural connections of OFC subregions with posterior OFC regions showing its densest connections to less cytoarchitecturally developed limbic and paralimbic regions, while the anterior OFC is more heavily connected with cytoarchitecturally well-developed cortical regions (Barbas and Pandya 1989; Carmichael and Price 1995a,1995b; Barbas 2000).

Conceptualizations of brain networks frequently emphasize the dynamic nature of functional connectivity. The level of functional connectivity between regions is presumed to vary depending upon the context, with network membership changing based on current perceptual, cognitive, or behavioral demands (Ioannides 2007). Within this framework, structural and resting-state functional measures cannot directly address the cognitive or perceptual context under which a given connection is meaningful. By contrast, because the MACM technique is based on task-related activations, it allows for an examination of functional connectivity within the context of specific task domains. We therefore additionally analyzed the pattern of coactivations after restricting the data to the specific task domains that show the most frequent engagement of the OFC. This approach allowed us to uniquely examine OFC functional connectivity within distinct cognitive and affective task domains.

Materials and Methods

Region of interest Definitions

To define search regions for the MACM, we manually defined a mOFC and a lOFC region of interest (ROI) on a T_1-weighted single-subject template (Holmes et al. 1998) using MRICro (http://www.cabiatl.com/mricro/). Given inconsistent accounts about potential OFC asymmetry, all ROIs were collapsed across hemisphere in order to increase statistical power.

The medial orbital sulcus (Fig. 1) was used as a primary divide between the mOFC and lOFC seed regions, with a maximum extension of the medial region equivalent to $x = \pm20$ at the point where the medial orbital gyrus bulges laterally. In the posterior extreme (behind the transverse orbital sulcus), the mOFC was limited to $x \le \pm14$, consistent with the curve of the caudal arm of the medial orbital sulcus (Chiavaras et al. 2001). The mOFC region was defined along y-axis from the posterior extreme of the OFC ($y = 6$) to $y = 60$ where the medial orbital gyrus and gyrus rectus are completely replaced by the frontomarginal gyrus (Mai et al. 1997). The ROI extended superiorly to $z = -16$, based on the average position of the rostral sulcus, and inferiorly to $z = -30$ to capture the ventral-most aspect of the gyrus rectus (Fig. 1).

The lOFC seed region was defined as the cortex lateral to the medial orbital sulcus, including the anterior and posterior orbital gyri, the lateral orbital gyrus, and the pars orbitalis portion of the inferior frontal gyrus, using the labeling scheme adopted by Chiavaras et al. (2001). The seed region included cortex lateral to $x = \pm24$ except in the more anterior portions of the region, which extended medially to as much as $x = \pm22$ in order to run parallel to the rostral limb of the medial orbital sulcus (Chiavaras et al. 2001). Along the y-axis, the region extended in the posterior direction to $y = 8$, at the posterior extreme of the lateral orbital gyrus, and anteriorly to the frontal pole at $y = 62$. Along the z-axis, the ROI began in its posterior-medial extreme at $z = -28$, corresponding to the ventral-most aspect of the posterior orbital gyrus, and ended its lateral extreme at $z = -8$ so as to include the inferior frontal gyrus (pars orbitalis), while excluding the triangularis sector of the inferior frontal gyrus.

For secondary analyses, we further split the medial and lateral regions into their respective anterior and posterior portions in order to determine whether greater regional specificity could be observed. For these analyses, the medial and lateral ROIs were split at a line running through the anterior-most point of the transverse orbital gyrus on the T_1-weighted MRI template at $y = 34$. This divide was selected based on its easy identification, and its correspondence to gross cytoarchitectural divisions in the human OFC (Petrides and Mackey 2006).

Meta-analytic connectivity modeling

The above anatomically defined ROIs in Montreal Neurological Institute (MNI) space were input as seed regions into the BrainMap (http://BrainMap.Org) database. BrainMap is a community accessible, electronic environment that stores the reported peak stereotactic coordinates for published functional neuroimaging studies, as well as information about the studies, such as the number of subjects, neuroimaging modality, and the functional domain and paradigm of the contrast (Laird, Eickhoff, Kurth et al. 2009; Laird et al. 2011). At the time of analysis, BrainMap archived 1913 papers, which included 8921 experiments reporting 71 192 brain activation locations. All contrasts in the BrainMap database that reported activation in the mOFC
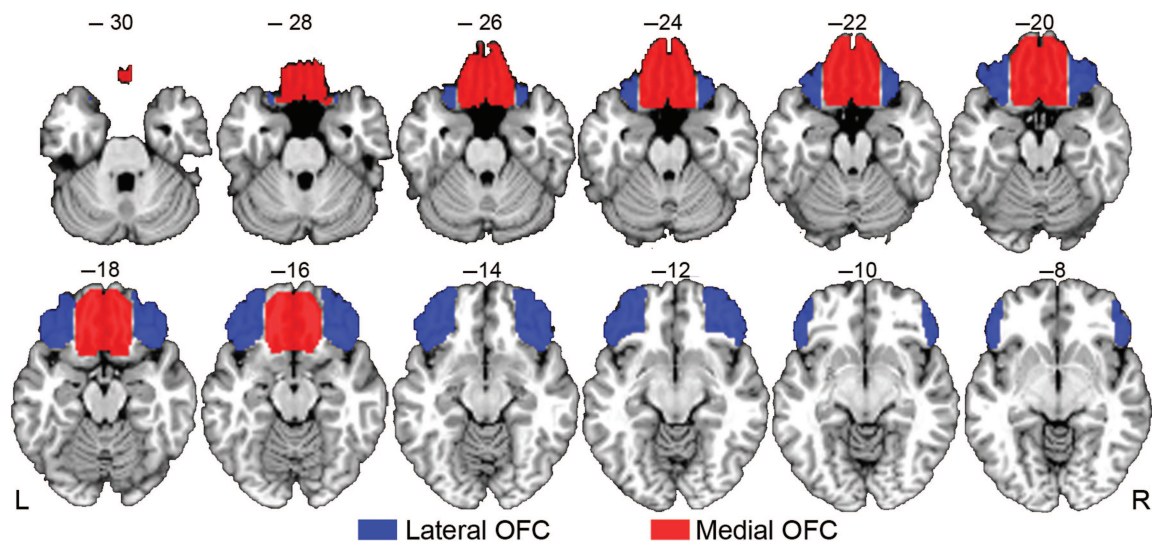
Figure 1. lOFC and mOFC seed ROIs for the MACM analysis displayed on the Colin T_1 MNI template. Slice numbers indicate MNI z coordinates.

or lOFC seed region were identified. Contrasts were limited to fMRI and positron emission tomography experiments reporting whole-brain activations (not deactivations) in healthy controls only; no search restrictions were made regarding the nature of task employed in each study. For any contrast that was found to possess activation in the seed region, the whole-brain coordinates of all activations arising in the contrast were identified and downloaded from the database for further analyses. Coordinates reported in Talairach space were converted to MNI space using the Lancaster (tal2icbm) transform algorithm (Lancaster et al. 2007; Laird et al. 2010).

To detect significant areas of coactivation, the modified activation likelihood estimation (ALE) algorithm (Eickhoff et al. 2009) was applied on the obtained coordinates. This approach models each focus as a Gaussian distribution reflecting empirical estimates of the uncertainty of different spatial normalization techniques. Rather than utilizing a user-defined full-width half maximum (FWHM) as in the original ALE approach (Turkeltaub et al. 2002), an algorithm was used to model the spatial uncertainty of each focus based on the estimation of the intersubject and interlaboratory variability typically observed in neuroimaging experiments (Eickhoff et al. 2009). This algorithm includes individual FWHM values for each experiment that are weighted by the sample size of the original study, thereby allowing experiments with larger numbers of subjects to be weighted more strongly than those with fewer subjects. For the present analyses, the minimum FWHM value used in the ALE calculations was 8.67 mm, the maximum value was 19.07 mm, and the mean value was 9.76 mm. ALE was performed using GingerALE 2.1 (Eickhoff et al. 2009). Modeled activation (MA) maps were computed by pooling all activation foci's probability distributions reported in a given experiment (Turkeltaub et al. 2012). The MA maps contain for each voxel the probability of activation being located at exactly that position in a given experiment. ALE scores were then calculated on a voxel-by-voxel basis by taking the union of these individual MA maps. Spatial inference on meta-analysis aims at identifying those voxels where the convergence across all MA maps is higher than expected if the results were independently distributed. The ALE scores were then tested for significance in a random-effects analysis against a null distribution reflecting a random spatial association between experiments (Eickhoff et al. 2012). Resultant ALE maps were thresholded to include only foci with a cluster-level threshold of $P_{corrected} < 0.01$ (corrected for family-wise error as described in Eickhoff et al. (2012) and converted to z-scores for visualization). In the resultant tables, labeling of orbital gyri and Brodmann numbering followed (Petrides and Mackey 2006).

Contrast Analysis

To determine whether regions showed significantly different levels of coactivation with the mOFC versus lOFC, we performed a contrast analysis that computed the voxel-wise difference between ALE scores for the 2 sets of coactivation foci (Eickhoff et al. 2011). The contributing experiments were pooled and randomly divided into 2 analogous sets of experiments of the same size as the 2 original sets. ALE scores for the randomized sets were computed, and the difference was recorded for each voxel in the brain. Repeating this process 10 000 times yielded a null distribution for the differences in ALE scores between the medial and lateral MACM analyses. The observed difference was then tested under this null distribution by thresholding for a posterior probability of $P > 0.99$ for true differences and additionally by masking with the significant main effect for $P_{corrected} < 0.01$ in the primary analysis for the seed region showing the larger ALE score.

Metadata Analysis

Metadata annotations are included in the BrainMap database to describe the behavioral paradigm or task that was employed in the published experiment. The paradigm class is assigned from a list of 81 choices and designed to maintain a well-structured taxonomy. For this study, the paradigm classes were restricted to the most robust subset of classes that included at least 50 reported experiments in the BrainMap database (the number of reported experiments for a given class ranged from 5 to 655 with an average value of 134 experiments). Imposing this limit restricted the paradigms in our metadata analysis

to 51 unique classes (this subset of paradigm classes is listed in Supplementary Table 1). We analyzed the metadata associated with the mOFC and lOFC ROIs to determine the frequency of paradigm classes activating a given region, relative to the distribution across the whole brain (i.e., the full database). For each OFC ROI, a chi-square test was performed to evaluate the regional distribution compared with the overall database distribution. If the region's distribution was significantly different, a binomial test was performed to determine which individual paradigms were overrepresented ($P < 0.05$, corrected for multiple comparisons using Bonferroni's method). This metadata analysis strategy identifies paradigms that result in an above-chance frequency of activation and was initially described by Laird, Eickhoff, Li (2009) in the context of behavioral domain metadata associated with regions in the default mode network.

Results

We identified 2922 mOFC activations in the BrainMap database. These mOFC activations arose in 251 contrasts from 176 studies with a total of 2922 subjects. We identified 7168 lOFC activations across 550 contrasts from 381 studies with a total of 6179 subjects. A list of the identified studies is included in Supplementary Materials.

ALE Results

Medial OFC Coactivations

We found significant coactivation with the mOFC along midline cortical and subcortical regions (Fig. 2, Table 1). A large bilateral cluster emerged that was centered in the ventromedial prefrontal cortex. Not surprisingly, the cluster centered on the area that was included in the mOFC seed region (suggesting that activations in this area are often co-occurring with other mOFC areas). The cluster also extended into ventral medial wall regions, including medial frontopolar as well as subgenual and pregenual cingulate cortex. The cluster also extended posteriorly to include subpeaks in the striatum (ventral striatum, ventral putamen, and ventromedial caudate), as well as the hypothalamus, amygdala, and hippocampus. Additional discrete cortical areas of coactivation occurred in the insula, presupplementary motor (preSMA) region of the superior frontal gyrus, as well as the middle and superior temporal gyri and planum temporale. The mOFC also demonstrated significant coactivations in the dorsomedial thalamus. Remarkably, there was little in the way of coactivation with more lOFC regions, with only one small cluster in each hemisphere appearing just anterior or posterior to the transverse orbital sulcus ($x = −38$, $y = 26$, $z = −20$, and $x = 36$, $y = 32$, $z = −16$). Similarly, there was only limited coactivation in lateral PFC regions, with the only coactivations occurring in small, circumscribed portions of the left inferior frontal gyrus [primarily Brodmann area (BA) 45] and the right middle frontal gyrus (approximately BA 46).

Lateral OFC Coactivations

The lOFC coactivated extensively with lateral prefrontal and dorsomedial frontal cortices and subcortical structures (Fig. 2, Table 2). As expected, a large bilateral cluster was centered on the lOFC. The area of coactivation extended broadly through the orbital, triangularis, and opercularis portions of the inferior frontal gyrus. More dorsally, the area included the posterior aspects of the dorsolateral prefrontal cortex in the middle frontal gyrus (BA 46/9), and, posterior to this, portions of lateral BA 6. A second large frontal cluster also
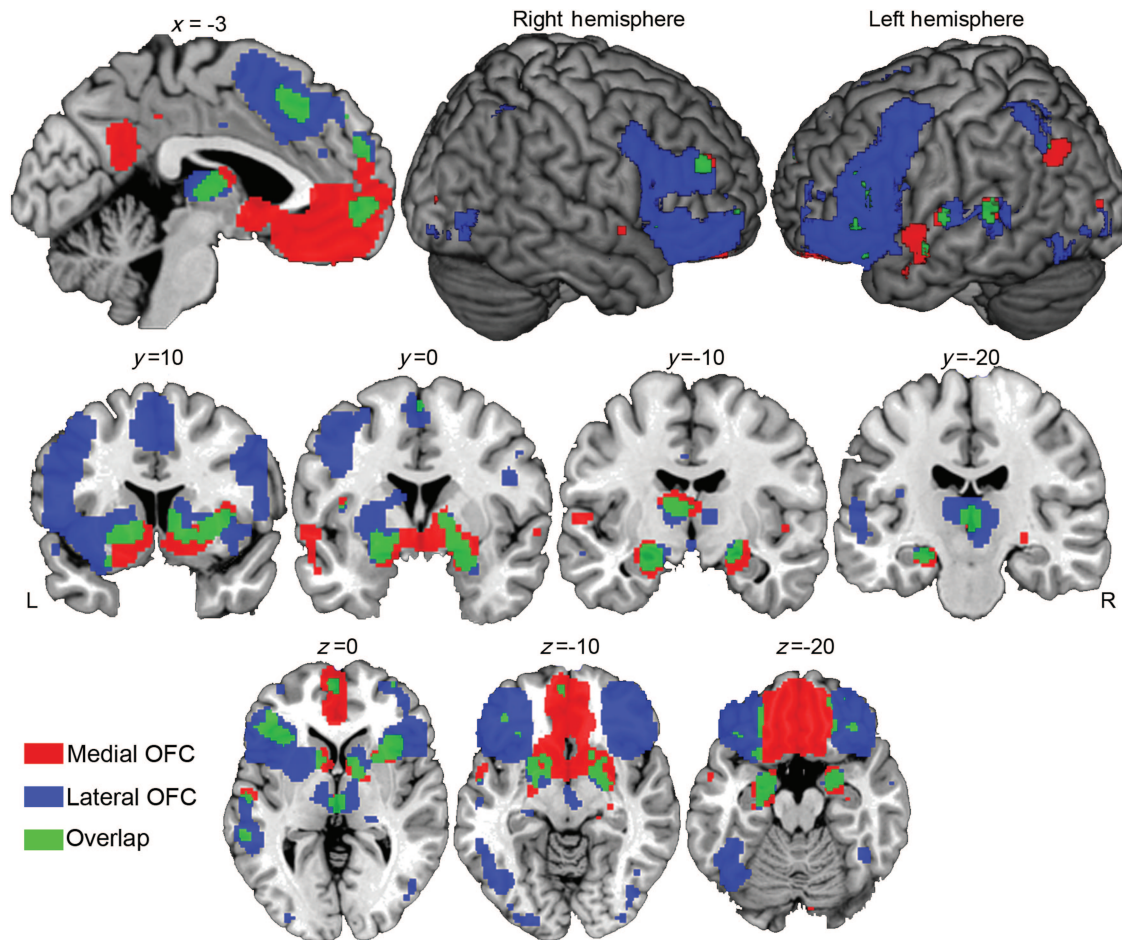
Figure 2. Areas showing significant coactivation with mOFC and lOFC seed ROIs. Areas in red indicate coactivation with mOFC; areas in blue indicate coactivation with lOFC. Areas in green indicate regions with overlapping mOFC and lOFC coactivation.

emerged on the dorsomedial wall along the medial portion of the superior frontal gyrus including medial BA 6 and BA 8, and the more superior aspects of the rostral cingulate. Subcortically, coactivations localized to the striatum (caudate and putamen) and into the medial temporal lobe (bilateral amygdala and left hippocampus). In terms of temporal cortex, there was striking coactivation of the left superior temporal gyrus, as well as aspects of the ventral visual stream including most notably the fusiform gyri and lateral occipital cortex. There was also strong coactivation of the bilateral thalamus. Remarkably, there was an almost complete absence of coactivations in the mOFC, with the only medial frontal area in the vicinity of the OFC occurring in the inferior-medial frontal pole (inferior rostral gyrus at $x = -2$, $y = 54$, $z = -4$).

Because the lOFC seed region included cortex both medial and lateral to the lateral orbital sulcus, in a supplemental analysis we examined to what extent overlapping patterns of coactivation emerged for seed regions limited to the more central OFC region (anterior and posterior orbital gyri medial to the lateral orbital sulcus), and the more extreme lateral segments of the OFC (lateral orbital gyrus and inferior frontal gyrus pars orbitalis, which lie lateral to the lateral orbital sulcus). $x = \pm 37$ served as the primary dividing line. Substantially, overlapping results emerged for the 2 subregions (Supplementary Fig. 1), although several areas showed preferential associations with the central or extreme lateral segments,

suggesting further parcellation based on functional connectivity is possible.

Conjunction Analysis

To determine the overlap between areas that were coactivated by both the lOFC and mOFC, we performed a logistic conjunction analysis to identify areas that were significantly coactivated with both mOFC and lOFC seed regions. These regions are displayed in green in Figure 2 and listed in Table 3. Several areas of the frontal lobe showed significant overlap between the mOFC and lOFC analyses. In particular, the left inferior frontal gyrus pars triangularis and medial frontal pole (inferior rostral gyrus) both showed large areas of overlap, while a smaller overlap emerged in the preSMA region of the superior frontal gyrus. The anterior insula also showed overlapping areas of coactivation bilaterally. In posterior cortical areas, overlap was observed in the planum temporale, superior temporal gyrus, and angular gyrus in the left hemisphere. Subcortically, clear areas of overlap emerged in the amygdala bilaterally (extending into the hippocampus in the left hemisphere), the dorsomedial thalamus, and the basal ganglia (ventromedial caudate, nucleus accumbens regions, ventral putamen, and globus pallidus).

In the OFC itself, there were only small regions that demonstrated coactivations with both the mOFC and lOFC seed regions. Specifically, discrete areas in the right and left central

Table 1
Clusters for mOFC coactivations

Cluster#	Region	Cluster volume (mm^3)	BA	X	Y	Z	ALE
1.	Bilateral gyrus rectus/ medial orbital gyrus/ medial frontopolar cortex	6734	11/14/10	0	48	−18	0.185
	Right medial orbital gyrus		13	14	32	−18	0.096
	Right amygdala			22	−4	−18	0.082
	Left amygdala			−22	−8	−18	0.081
	Left pregenual cingulate		32	0	42	0	0.073
	Left frontal pole		10	−2	62	2	0.072
	Right ventral striatum			10	6	−10	0.069
	Right anterior insula			34	16	2	0.063
	Left ventral striatum			−8	6	−6	0.057
	Left ventral striatum			−12	12	−6	0.056
	Left putamen			−16	10	−10	0.056
	Right caudate			10	6	2	0.054
	Left (medial) superior frontal gyrus		9	−8	56	20	0.049
	Right putamen			26	10	−4	0.046
	Right anterior orbital gyrus		11/10	28	50	−16	0.04
2	Right posterior cingulate	5448	23	4	−52	26	0.063
	Left precuneus		23	−6	−56	20	0.056
	Right posterior cingulate		30	4	−50	18	0.053
3	Right thalamus	3416		2	−18	10	0.052
	Left thalamus			−10	−12	10	0.048
4	Left anterior insula	3112		−32	24	−4	0.06
5	Bilateral (medial) superior frontal gyrus	2072	32	−2	24	42	0.059
6	Left superior temporal gyrus	1304	22	−56	0	−6	0.047
	Left middle temporal gyrus		21	−52	2	−26	0.038
7	Left middle frontal gyrus	1304	46	−42	26	18	0.041
	Left inferior frontal gyrus (pars triangularis)		45	−52	22	10	0.04
8	Left superior temporal gyrus	1128	22	−64	−36	8	0.05
	Left middle temporal gyrus		21	−60	−38	−2	0.048
9	Left angular gyrus	824	39	−48	−68	30	0.045
10	Left posterior cingulate	760	31	0	−36	38	0.045
11	Left transverse temporal gyrus	736	22	−56	−14	2	0.047
12	Right middle frontal gyrus	560	46	42	42	26	0.045
13	Right lateral orbital gyrus	408	47/12	36	34	−14	0.041
14	Right parietal operculum	304		44	−24	16	0.041

Coordinates identify local maxima in MNI space.

OFC ($x = 36$, $y = 32$, $z = −16$; $−x = 38$, $y = 26$, $z = −20$) coactivated in both analyses. A small area along the medial orbital sulcus was also observed for both seed regions, but likely, at least partially reflects an artifact of spatial smoothing along the boundary of the 2 seed regions.

Contrast Analysis

To determine whether regions showed significantly different levels of coactivation with the mOFC versus lOFC, we performed a contrast analysis that computed the voxel-wise difference between ALE scores for the 2 sets of coactivation foci (Eickhoff et al. 2011). Table 4 lists the locations of areas that were significantly more frequently coactivated with the mOFC than the lOFC and that are displayed in Figure 3. The coactivations are naturally a subset of those observed in the primary analysis of the mOFC. Not surprisingly, a large ventromedial region showed significantly greater coactivation with the mOFC than the lOFC. A smaller peak also emerged in the medial frontal pole. Outside of the frontal cortex, the

retrosplenial cortex and posterior cingulate showed significantly more coactivation than the lOFC. Additionally, a midline area including a part of the ventral striatum and hypothalamus/basal forebrain also emerged. A cluster of voxels in the right medial temporal lobe hippocampus and amygdala also showed preferential coactivation with the mOFC.

Areas showing greater coactivation with the lOFC than the mOFC are listed in Table 5 and displayed in Figure 3. Most of the regions that showed significant coactivation with the lOFC in the primary ALE analysis demonstrated significantly greater levels of coactivation with the lOFC than the mOFC. This was evident in frontal regions including the right and left ventrolateral areas extending dorsally through the posterior sectors of the inferior frontal gyrus and precentral gyrus, portions of the dorsolateral prefrontal cortex (middle frontal gyrus), and the left cingulate/preSMA region. Several additional discrete areas showed greater coactivation with the lOFC than the mOFC, including the left insula/claustrum/lateral putamen, ventral visual stream areas in the temporal lobe including the fusiform gyrus, along the left superior temporal sulcus, and portions of the inferior and superior parietal lobule.

Anterior–Posterior Differences

To assess the differences between anterior and posterior OFC regions, we separately divided the mOFC and lOFC into anterior and posterior sectors. After deriving separate ALE maps for each of these sectors we performed contrast analyses using identical methods as described above for the lateral versus medial contrast. Outside of the seed regions themselves, only a small number of regions showed statistically significant differences in the anterior versus posterior contrasts. These are described below and detailed in Tables 6 and 7.

For the mOFC, the posterior sector showed a significantly greater association with a large cluster that extended from the posterior mOFC and subgenual cingulate posteriorly along the midline to the hypothalamus. The posterior mOFC additionally showed a significantly stronger association with the right insula and dorsomedial thalamus. Finally, the posterior mOFC was uniquely associated with the cerebellum (along the midline in the tuber of the vermis and declive). Conversely, the anterior mOFC showed coactivations that extended dorsally to occupy portions of the medial frontal pole. The anterior mOFC also showed distinct coactivation with a medial section of the superior frontal gyrus.

In the lOFC, the posterior division showed significantly greater associations than the anterior division with the left inferior frontal gyrus pars triangularis, the right precentral gyrus, and the left uncus proximal to the amygdala. In both hemispheres, the large cluster falling in the posterior lOFC seed region also extended posteriorly to include primary pyriform cortex near the boundary of the temporal and frontal lobes. In contrast, the anterior sector of the lOFC showed more associations than the posterior sector in an area extending from the lOFC seed region to lateral elements of the frontal pole (middle frontal gyrus). The anterior sector also showed a significant association with the left intraparietal suclus region.

Metadata Analysis

Of the 51 classes of paradigms categorized in the BrainMap database, several classes produced frequent activations of the OFC. Figure 4A displays the 20 paradigms that produced the

Table 2
Clusters for lOFC coactivations

Cluster #	Region	Cluster volume (mm³)	BA	X	Y	Z	ALE
1	Left inferior frontal gyrus/lateral orbital gyrus	135 656	47/12	−46	26	−8	0.348
	Right posterior/lateral orbital gyrus		13/47	40	26	−12	0.274
	Left insula			−34	22	−2	0.224
	Left inferior frontal gyrus (pars opercularis)		44	−48	20	20	0.208
	Right anterior orbital gyrus		11	34	48	−14	0.155
	Left precentral gyrus		6	−48	8	32	0.145
	Right inferior frontopolar cortex		10	44	46	−8	0.143
	Left middle frontal gyrus		6	−40	6	44	0.131
	Right middle frontal gyrus		46	50	28	20	0.12
	Left putamen			−26	4	−2	0.12
	Left inferior frontal gyrus (pars opercularis)		44	−52	14	6	0.118
	Left amygdala			−18	−6	−16	0.114
	Left thalamus			−8	−14	6	0.114
	Right precentral gyrus		6	46	8	30	0.108
	Left putamen			−18	12	−4	0.102
	Right amygdala			22	−4	−16	0.101
	Right thalamus			6	−18	4	0.099
	Right middle frontal gyrus		46	44	40	20	0.095
	Right caudate			12	10	−2	0.095
	Right inferior frontal gyrus (pars triangularis)		45	56	14	8	0.083
	Left middle frontal gyrus		10	−36	50	10	0.078
	Left hippocampus			−24	−22	−16	0.077
	Left caudate			−12	2	12	0.075
	Left middle frontal gyrus		6	−28	2	56	0.074
	Left midbrain			0	−12	−12	0.07
	Right thalamus			10	−6	4	0.07
	Left insula			−38	2	8	0.067
2	Left (medial) superior frontal gyrus	23 360	6	−2	12	52	0.182
	Bilateral (medial) superior frontal gyrus		8/6	0	20	44	0.178
	Bilateral (medial) superior frontal gyrus		9	0	42	30	0.068
3	Left middle temporal gyrus/superior temporal sulcus	15 536	22	−56	−40	0	0.137
	Left lateral occipital cortex		19	−42	−68	−12	0.119
	Left occipital gyrus			−46	−54	−18	0.106
	Left planum temporale		41	−60	−16	4	0.087
	Left superior temporal gyrus/superior temporal sulcus		22	−54	−18	−6	0.074
	Left cerebellum			−30	−62	−24	0.068
4	Left intraparietal sulcus	6976	7	−30	−56	48	0.134
	Left angular gyrus		39	−48	−62	38	0.07
5	Right intraparietal sulcus	1864	7	36	−54	48	0.082
	Right angular gyrus		39	34	−62	46	0.081
6	Left (medial) superior frontal gyrus	1320	9	−6	56	24	0.088
7	Left rostral frontal gyrus	1296	8/32	−2	54	−4	0.082
8	Right lateral occipital cortex	1192	19	42	−76	−10	0.074
	Right occipital gyrus		18	48	−72	0	0.071
	Right occipital gyrus		18	34	−92	−10	0.066
9	Left occipital pole	1104	18	−28	−94	−6	0.08
10	Right fusiform gyrus	832	37	44	−52	−20	0.079
	Right inferior temporal gyrus		37	42	−60	−14	0.066
11	Right thalamus	384		22	−28	−4	0.075

most frequent OFC activations as a percentage of all studies reporting OFC activation (calculated separately for mOFC and lOFC seed ROIs). OFC activations most frequently arose for the paradigm classes of reward, face, and semantic monitoring/discrimination tasks. They also frequently emerged for memory-related tasks: Cued explicit recognition was the fourth most frequent class, while episodic recall, encoding, and paired recall also appeared in the top 20 classes producing OFC activations. We note that this analysis does not correct for differences in the number of studies within a given paradigm in the BrainMap database. Therefore, paradigms that are more frequently studied in the neuroimaging literature may be over-represented relative to less frequently studied paradigms. To control for this bias, Figure 4B shows the top 20 paradigms with OFC activations as the percentage of all studies for each paradigm class. As can be seen in Figure 4B, a high percentage of tasks involving deception, eating and drinking, music comprehension/production, and olfactory monitoring/discrimination produced OFC activations, but because these classes of paradigms are less numerous in the BrainMap database, they fall lower in the list in Figure 4A.

We performed a chi-square test to reveal whether each paradigm class was observed significantly more frequently for the mOFC or lOFC relative to the whole-brain distribution of activations for the given paradigms. Binomial tests of individual paradigm classes revealed that several classes were observed at frequencies higher than what would be expected compared with the distribution across the whole brain. mOFC activations occurred significantly more frequently than expected by chance for tasks involving reward ($P_{corrected} < 0.0001$), eating and drinking ($P_c < 0.0004$), and music comprehension and production ($P_c < 0.0005$). In contrast, deception ($P_c < 0.0195$) and semantic monitoring/discrimination ($P_c < 0.0100$) tasks caused lOFC activations at a greater level than expected by chance.

Paradigm-Specific Analyses

To examine task-specific functional connectivity, data from the 3 paradigm classes with the most frequent activations in the OFC were independently submitted to MACM analysis. We additionally performed a MACM analysis on memory retrieval tasks by collapsing the cued explicit recognition, episodic recall, and paired associated recall paradigm classes (which when taken together had the highest number of OFC activations).

Reward Tasks

A total of 674 foci from 58 experiments in 41 studies utilizing reward tasks localized to the lOFC, while 480 foci from 60 experiments in 38 papers localized to the mOFC. The lOFC and mOFC showed several areas with convergent coactivations during reward tasks (Fig. 5a and Table 8). Of particular note, there were common areas of coactivations within the OFC itself, which were not present in the other functional domains studied. Beyond the OFC, both medial and lateral sections of the OFC demonstrated coactivations in the ventral striatum, with the lOFC's pattern falling slightly superior to the mOFC's, but with a large area of overlap throughout the

regions containing the nucleus accumbens. Overlapping mOFC and lOFC coactivations additionally localized to the amygdala and a small area of the ventral visual cortex. Outside of the OFC itself, coactivations specific to either the mOFC or lOFC were generally small in volume. Notably, the lOFC showed coactivation in the midline dopaminergic midbrain (ventral tegmental area), which was not observed in the other functional domains examined.

Memory

Collapsing across the different memory categories, we observed 1590 foci in the lOFC derived from 104 experiments in 74 papers and 485 foci in the mOFC from 31 experiments across 25 papers. The lOFC exhibited extensive coactivations in the inferior frontal gyrus bilaterally and parts of the middle frontal gyrus as well as the preSMA/SMA region (Fig. 5B and Table 9). We found subcortical coactivations with the lOFC in the left hippocampus, medial thalamus, and dorsal head of the caudate. Within the OFC itself, there was minimal overlap between the areas showing coactivation with the mOFC and lOFC (with the lOFC coactivations focused throughout the lOFC, and the mOFC coactivations restricted to the most anterior-medial segments of the OFC). The mOFC showed more restricted cortical coactivations than the lOFC, with small areas of overlap in the preSMA/SMA and left inferior frontal regions. By contrast, the mOFC was differentially coactivated with the bilateral amygdala and right anterior hippocampus. All other coactivations with the mOFC were small in extent.

Face Processing

A total of 415 foci from 34 experiments across 24 papers localized to the lOFC during face processing and 16 papers reported mOFC activation with 187 foci from 21 experiments. Coactivations for the lOFC and mOFC were largely divergent for the face domain. In the prefrontal cortex, lOFC coactivated with inferior frontal gyrus pars orbitalis, whereas mOFC coactivations were found in the gyrus rectus and subcallosal region (Fig. 5C and Table 10). The lOFC showed 2 notable coactivations in the amygdala and the right fusiform gyrus, both of which are known to participate in face processing. By contrast, the mOFC showed coactivation centered more on the hippocampus and did not show any association with the fusiform gyrus.

Table 3

Areas of overlapping mOFC–lOFC coactivation

Region	BA	X	Y	Z
Left amygdala		−18	−2	−12
Left transverse orbital sulcus	11/13	−24	30	−18
Left lateral orbital gyrus	47/12	−38	26	−20
Left superior temporal gyrus	22	−56	−6	−14
Left occipital gyrus	19	−42	−74	−12
Left inferior frontal gyrus (pars orbitalis)	47/12	−38	28	−2
Left inferior rostral gyrus	10	−2	54	−4
Left middle temporal gyrus	21	−60	−38	0
Left thalamus		−4	−14	6
Left planum temporale		−58	−14	2
Left middle frontal gyrus	9	−46	24	16
Left insula		−38	0	8
Left superior frontal gyrus	10	−6	56	24
Left angular gyrus	39	−44	−66	36
Left (medial) superior frontal gyrus	6/8	−2	24	44
Left superior frontal gyrus	9	−4	48	38
Bilateral (medial) superior frontal gyrus	6	0	−2	58
Right putamen		24	8	−6
Right transverse orbital sulcus	13/11	36	32	−16
Right medial orbital gyrus	11	24	42	−16
Right middle frontal gyrus	10	36	58	0
Right middle frontal gyrus	10/46	42	40	24

Coordinates reflect centroids of clusters for mOFC–lOFC logistic analysis.

Table 4

Contrast analysis: mOFC > lOFC

Cluster#	Region	Cluster volume (mm³)	BA	X	Y	Z	ALE
1	Bilateral gyrus rectus/medial orbital gyrus/inferior rostral gyrus	38 136	11/13/14/25/32	0	36	−18	3.719
	Hypothalamus/ventral striatum/basal forebrain			3	6	−6	3.353
	Right ventral striatum/globus pallidus			8	5	−10	3.239
	Right ventral striatum/globus pallidus			10	4	−6	3.156
2	Right retrosplenial cortex	4184	29/30	5	−51	20	3.719
	Left retrosplenial cortex		30	−10	−54	16	3.54
	Left retrosplenial cortex		31	−4	−58	32	2.794
3	Medial frontopolar cortex	848	10	0	65	3	3.719
4	Right hippocampus	728		32	−14	−18	3.156
	Right amygdala			26	0	−12	2.848
5	Left angular gyrus	344	39	−48	−72	32	3.54
6	Left posterior cingulate gyrus	336	31	−2	−34	38	2.794
	Bilateral posterior cingulate gyrus		31	0	−30	38	2.748
	Right posterior cingulate gyrus		31	4	−26	40	2.605
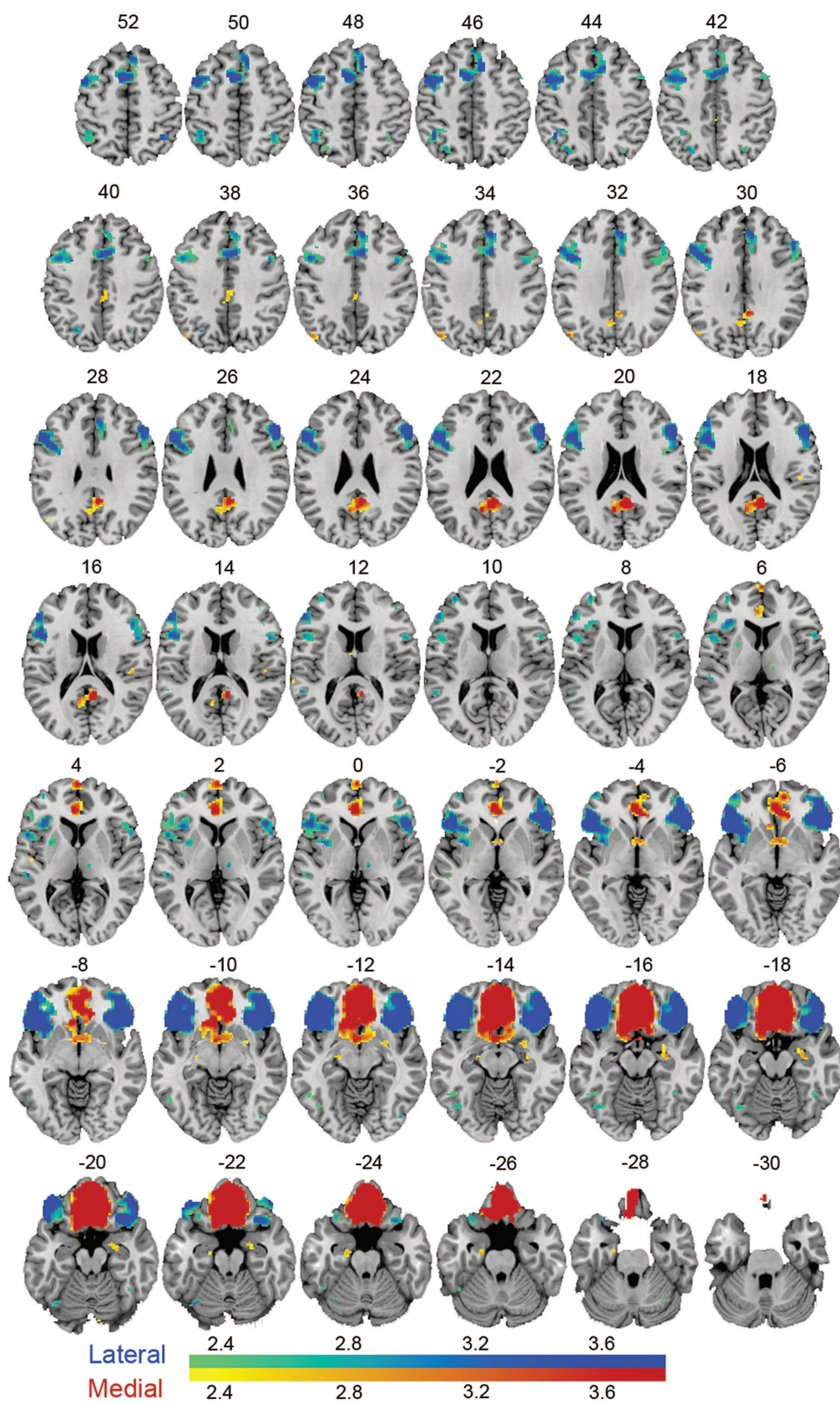
Figure 3. Regions showing statistically significant differences in the frequency of coactivation between the lOFC and mOFC seed regions. The color scale reflects the magnitude of the difference with areas in green to blue showing significantly greater coactivation with the lOFC, and areas in yellow to red showing significantly greater coactivation with the mOFC.

Table 5
Contrast analysis: lOFC > mOFC

Cluster#	Region	Cluster volume (mm³)	BA	X	Y	Z	ALE
1	Left inferior frontal gyrus (pars orbitalis)/lateral orbital gyrus	37 232	47/12	−44	28	−5	3.719
	Left insula			−34	12	8	3.54
	Left frontal operculum/precentral gyrus		6/44	−53	12	4	3.353
	Left middle frontal gyrus		10	−36	54	8	3.156
	Left posterior orbital gyrus		13	−30	20	−28	3.036
	Left frontal operculum/precentral gyrus		44	−46	8	6	2.948
	Left posterior orbital gyrus		13	−30	24	−26	2.911
	Left middle frontal gyrus		9	−40	22	34	2.848
	Left middle frontal gyrus		6	−28	4	56	2.706
2	Right inferior frontal gyrus (pars opercularis)	25 608	47/12	44	30	−8	3.719
	Right middle frontal gyrus		46	48	26	28	3.54
	Right inferior frontal gyrus (pars opercularis/triangularis)		44/45	45	15	16	3.239
	Right inferior frontal gyrus (pars opercularis)		44	55	12	12	3.156
	Right middle frontal gyrus		6	52	10	44	2.848
	Right inferior frontal gyrus (pars opercularis)		44	44	2	20	2.409
3	Bilateral (medial) superior frontal gyrus	11 216	6/8	0	16	46	3.719
	Right (medial) superior frontal gyrus		8	9	19	47	3.54
	Bilateral (medial) superior frontal gyrus		8	1	32	49	3.353
4	Left inferior parietal lobule	1512	40	−40	−52	44	3.719
	Left inferior parietal lobule		40	−42	−48	50	3.156
	Left intraparietal sulcus		40	−32	−46	44	3.036
5	Cerebellum	560		−36	−68	−22	3.239
	Cerebellum			−32	−66	−22	2.989
	Left fusiform gyrus		37	−42	−66	−14	2.948
6	Left superior parietal lobule	520	7	−28	−66	42	3.239
7	Left fusiform gyrus	408	37	−43	−52	−26	2.652
	Left inferior temporal gyrus		37	−52	−54	−14	2.576
	Left inferior temporal gyrus		37	−53	−59	−9	2.549
	Left inferior temporal gyrus		37	−44	−54	−16	2.524
	Left inferior temporal gyrus		37	−48	−54	−14	2.512
	Left fusiform gyrus		37	−42	−48	−24	2.447
8	Right intraparietal sulcus	328	7	37	−52	52	3.719
	Right superior parietal lobule		7	36	−56	52	3.54
9	Left superior temporal gyrus	304	22	−52	−30	2	3.54

Table 6
Significant differences between anterior versus posterior sectors of the mOFC

Cluster#	Region	Cluster volume (mm³)	BA	X	Y	Z
Anterior > posterior						
1	Bilateral gyrus rectus/inferior frontal pole	17 480	11m/10	2	50	−18
	Left anterior orbital gyrus		11	−26	48	−14
2	Right frontal pole	848	10	37	55	−6
3	Left anterior orbital gyrus	296	11	−36	36	−18
	Right anterior orbital gyrus		11	−34	34	−14
4	Left superior frontal gyrus	272	8	−8	40	40
Posterior > anterior						
1	Bilateral gyrus rectus (extending posteriorly to hypothalamus)	20 752	14	−2	20	−20
	Right posterior orbital gyrus/anterior claustrum		13	24	16	−8
2	Right anterior insula	1576		36	5	1
	Right anterior insula			34	4	6
	Right anterior insula			34	0	8
	Right anterior insula			38	4	−8
3	Left dorsomedial thalamus	704		−4	−26	6
	Right dorsomedial thalamus			6	−16	6
4	Cerebellum (vermis)	656		2	−72	−23
	Cerebellum (declive)			3	−68	−14

Table 7
Significant differences between anterior versus posterior sectors of the lOFC

| Cluster#	Region	Cluster volume (mm³)	BA	X	Y	Z
Anterior > posterior						
1	Right anterior/lateral orbital gyrus	15 312	11	34	50	−12
	Right middle frontal gyrus		10	39	48	7
2	Left anterior/lateral orbital gyrus	12 488	11	−34	47	−13
3	Left intraparietal sulcus	2416	7	−32	−58	44
Posterior > anterior						
1	Left posterior/lateral orbital gyrus	11 072	12/47	−34	22	−18
2	Right posterior/lateral orbital gyrus	8280	12/47	34	23	−19
3	Left inferior frontal gyrus (pars triangularis)	528	45	−54	28	4
	Left inferior frontal gyrus (pars triangularis)		45	−54	26	0
4	Right frontal operculum/precentral gyrus	372	6	44	2	26
5	Left uncus	352	34	−12	−4	−16

Semantic Monitoring/Discrimination

Five hundred sixty-four foci from 55 experiments in 37 studies arose in the lOFC during studies with semantic processing. Substantial coactivation occurred with language-related cortex in the inferior frontal gyrus and frontal operculum (in the left hemisphere (Fig. 5D and Table 11). Coactivations also occurred in areas frequently associated with language and auditory processing, including portions of the middle temporal gyrus (BA 21) as well as portions of the superior temporal gyrus (BA 22) and the angular gyrus (BA 39), further highlighting the lOFC's involvement with a language network. Coactivations with the mOFC are displayed in Figure 5C. Because only 10 studies reported mOFC activations during semantic processing, these results should be treated with caution and are not discussed further.
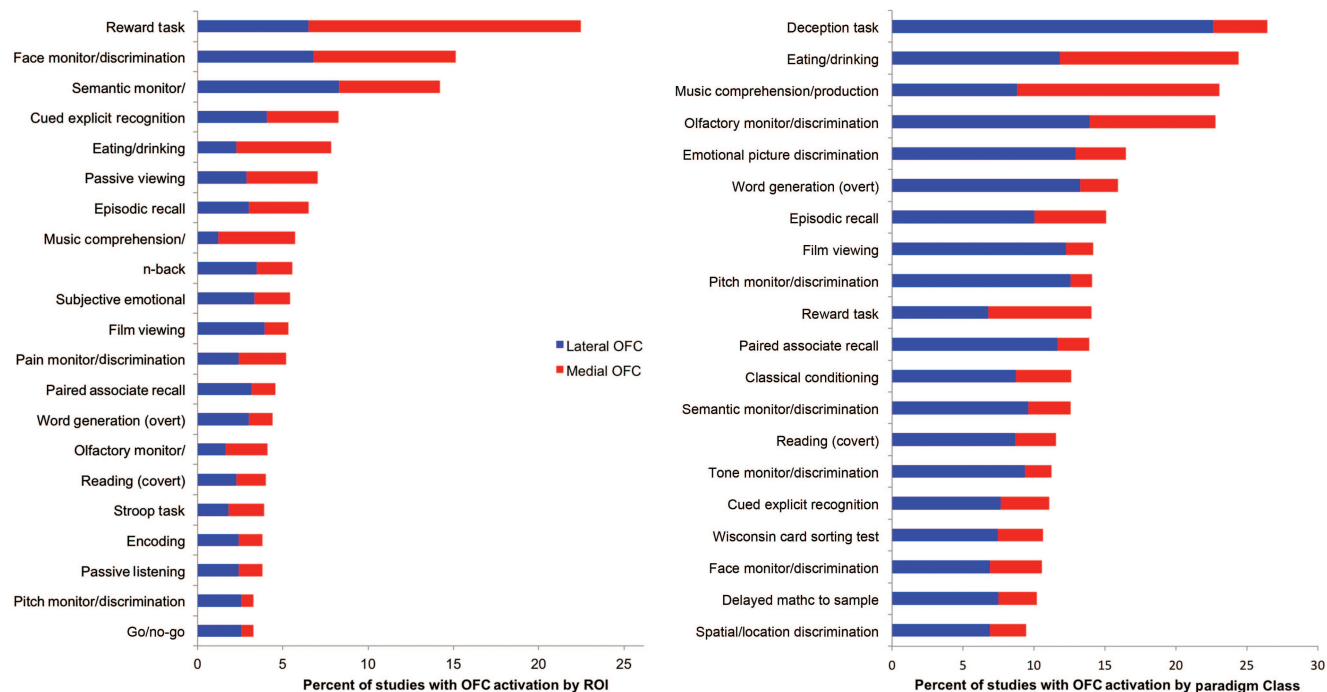
Figure 4. Top 20 paradigm classes with reported OFC activation (*A*) as a percentage of all studies reporting OFC activation and (*B*) as a percentage of paradigm class. Asterisks indicate paradigm classes for which OFC activations occurred more frequently than predicted by chance relative to the whole-brain distribution of activations for the given paradigm.

Discussion

The present application of the MACM technique revealed several notable features of the task-based functional connectivity of the human OFC. Many of these features converge with findings from other methodologies such as tract-tracing studies in animals and resting-state functional connectivity in humans. However, MACM also revealed several unique features of large-scale networks involving the OFC that have not been previously articulated and may influence future thinking about the OFC.

Segregation of mOFC and lOFC Circuits

Overall, the results of the MACM analyses indicate a strong segregation between mOFC and lOFC regions with only restricted areas of coactivation with the mOFC seed falling within the lOFC region and vice versa. This segregation finds parallels in both lesion studies and human neuroimaging studies that often emphasize distinct behavioral correlates of the mOFC and lOFC (Zald and Kim 1996b; Kringelbach and Rolls 2004). Describing the connections of the OFC in nonhuman primates, Carmichael and Price (1996) emphasize 2 distinct networks in the orbital and medial prefrontal cortex based on the density of connections between frontal subregions. They define a medial network (which includes areas 14 and 11m on the ventral surface of the frontal lobe and all of the medial wall, including Walker's areas 11m, and 25, 32, 10m, 24a, 24b, and 9), and an orbital network that is focused on more central aspects of the OFC (Walker's areas 13m, 13l, 11, and 12m). We did not attempt to create seed regions that specifically matched Carmichael and Price's division between medial and orbital networks in the absence of probabilistically defined boundaries of human OFC subregions. Nevertheless, our topographically defined mOFC seed region overlaps significantly with parts of Carmichael and Price's medial network, while our lOFC seed region includes a substantial part of Carmichael and Prices orbital network. Not surprisingly given this overlap, task-based functional connectivity often recapitulated aspects of the known structural connectivity of the medial and orbital networks. For instance, the mOFC seed showed strong coactivations with ventral medial frontal wall regions, whereas the lOFC seed was largely devoid of coactivations with those inferior-medial wall regions. In further support of the mOFC/lOFC division, Kahnt et al. (2012) used a clustering algorithm to demarcate OFC subdivisions based on resting-state functional connectivity. Despite different methods of OFC segregation and resting state rather than task-based data, they found a broad separation between mOFC and lOFC connectivity as in the present results.

Carmichael and Price label several subregions on the orbital surface as intermediate in that they possess afferent and efferent connections with both the medial and orbital networks (e. g., 13a and 13b whose homolog falls in our mOFC seed region, and area 12o whose homolog lies in our lOFC seed region). The presence of such intermediate areas within our seed regions would have been predicted to lead to regionally-specific coactivations across the 2 seed regions. However, to the limited extent that such cross-regional coactivations occur, they did not appear to align with the human homologs of Carmichael and Price's intermediate regions. Future studies will be necessary to clarify whether these differences arise due to cross-species factors or differences in the methods for defining structural versus functional connectivity.

Among the 4 task domains analyzed in isolation, only reward-related tasks led to significant coactivation of mOFC and lOFC regions, with distinct coactivations arising in a central region just posterior to the transverse orbital sulcus, a

Table 8
Behavioral domain analysis: Reward

Cluster#	Region	Cluster volume (mm³)	BA	X	Y	Z	ALE
lOFC							
1	Left putamen	9696		−14	10	−6	0.048
	Left anterior insula			−28	26	−10	0.044
	Left medial orbital gyrus		11	−18	40	−16	0.037
	Left posterior orbital gyrus		13	−28	22	−20	0.034
2	Right caudate	4072		12	12	−4	0.053
	Right amygdala			22	−2	−16	0.028
3	Right anterior insula	3592		38	18	−6	0.045
	Right anterior insula			32	22	−12	0.04
	Right lateral orbital gyrus		47/12	44	34	−14	0.025
4	Right anterior orbital gyrus	2336	11	24	46	−16	0.037
	Right middle frontal gyrus		10	40	54	−10	0.035
5	Left inferior occipital gyrus	872	18	−26	−94	−12	0.039
6	Left middle frontal gyrus	816	10	−34	54	−14	0.042
7	Left paracingulate gyrus	552	32	0	30	32	0.031
8	Right thalamus	512		2	−18	12	0.031
9	Right inferior occipital gyrus	424	18	32	−92	−10	0.024
10	Left (medial) superior frontal gyrus	408	6	0	24	42	0.026
11	Left anterior cingulate gyrus	360	32	−2	42	12	0.026
12	Left ventral tegmental area	352		0	−16	−14	0.025
	Right ventral tegmental area			4	−16	−12	0.024
13	Left superior parietal lobule	320	7	−30	−58	48	0.029
mOFC							
1	Bilateral gyrus rectus	24 360	14	0	34	−20	0.070
	Left medial orbital gyrus	0	11	−16	40	−16	0.046
	Right nucleus accumbens	0		12	10	−10	0.033
	Right medial frontopolar gyrus	0	10	4	54	−4	0.027
	Left anterior insula	0		−28	24	−8	0.026
	Right caudate	0		16	18	0	0.025
	Right amygdala	0		22	−2	−18	0.024
	Right caudate	0		6	18	6	0.022
	Left insula	0		−32	18	6	0.019
2	Left putamen	3280		−16	8	−12	0.037
	Left caudate	0		−6	14	4	0.022
3	Right posterior cingulate gyrus	2568	30	6	−50	18	0.035
	Left posterior cingulate gyrus	0	30	−6	−54	16	0.026
4	Left occipital gyrus	784	18	−26	−94	−14	0.030
5	Left anterior orbital gyrus	624	10	−34	54	−12	0.031
6	Right lateral orbital gyrus	528	47/12	30	28	−14	0.024

region near the junction of the OFC and insula, and in a small anterior-lateral region. Thus, it would be wrong to conclude that there is no common activation of mOFC and lOFC regions: Rather coactivations appear restricted in terms of both tasks and the specific subregions in question.

In considering the limited coactivations between the mOFC and lOFC, it is worth noting that the approach utilized here was exclusively focused on positive patterns of covariance. If activity in areas were inversely related, such that one area routinely suppresses activity in the other area, we would not be able to detect it in the analyses performed here. There are indeed some examples in the published literature where activity in the lOFC and mOFC appears to act in an opposite fashion with mOFC areas increasing with rewards, while lOFC increases with a decreasing reward value or negative outcomes, such as monetary loss (for example, Small et al. 2001; Kringelbach and Rolls 2004; O'Doherty and Dolan 2006). Future MACM analyses that include both positive and negative contrasts could complement the current analysis to

clarify if the mOFC and lOFC show activity that under some conditions is in fact anticorrelated rather than being largely independent as suggested by the present analyses.

Functional Connectivity with Lateral and Dorsomedial Prefrontal Regions

The segregation of the mOFC and lOFC was also apparent in terms of connectivity with other frontal regions. The lOFC showed significantly greater coactivation than the mOFC with all portions of the inferior frontal gyrus, the posterior aspects of the dorsolateral prefrontal cortex, and portions of premotor cortex (area 6). The greater connectivity of lOFC to the lateral prefrontal regions is not surprising given the existing literature on the patterns of structural connectivity within the primate prefrontal cortex (Barbas and Pandya 1989; Carmichael and Price 1996; Petrides and Pandya 2002), although the spatial extent of coactivations with the lOFC extend beyond areas that are usually emphasized in considering the circuitry of the OFC.

The level of coactivation within language-related areas of the inferior frontal gyrus (particularly the opercularis region) is particularly notable given that our lOFC seed region did not extend dorsally into more traditionally defined language areas of the inferior frontal gyrus. This coactivation appeared primarily driven by studies involving semantic monitoring and discrimination. Consistent with this pattern of coactivation, the metadata analysis revealed that semantic monitoring and discrimination tasks caused lOFC activations significantly more frequently than expected by chance. The lOFC also was associated with discrete foci in the left superior temporal sulcus in areas often engaged during language tasks (Dehaene et al. 1997). These tasks were not limited to studies involving emotional stimuli, but rather included basic tasks such as judgments of semantic plausibility and naming (Bookheimer et al. 1995; Papathanassiou et al. 2000; Luke et al. 2002; Vanlancker-Sidtis et al. 2003). The present findings converge with a study by Bokde et al. (2001), who examined functional connectivity of different inferior frontal gyrus regions during word processing, and observed significant functional connectivity extending into the lateral orbital regions. Such data suggests that the semantic processing zones of the prefrontal cortex extend further ventrally than is often appreciated in the literature.

While the ventral medial wall showed a preferential coactivation with the mOFC, consistent with the medial network described by Carmichael and Price, the pattern in more dorsal medial wall areas was more complex. Both lOFC and mOFC showed coactivation with a region near the boundary of the anterior cingulate (BA 32) and the superior (medial) frontal gyrus. However, the lOFC showed a significantly broader pattern of dorsomedial coactivation, which extended to include much of area 6 and 8 along the medial wall of the superior frontal gyrus and included the preSMA region. These areas are not typically emphasized in discussions of OFC networks. However, in studies with rhesus monkeys, Bates and Goldman-Rakic (1993) described significant connections between lOFC areas (Walker's 12 and more lateral aspects of area 11) and medial premotor regions. These areas have garnered significant functional attention given their role in a number of cognitive regulation tasks (Ridderinkhof et al. 2004). Both dorsomedial regions and a ventrolateral prefrontal area centered on the inferior frontal gyrus have been posited to form core nodes in a network involved in response

Table 9

Behavioral domain analysis: Memory

Cluster#	Region	Cluster volume (mm³)	BA	X	Y	Z	ALE
lOFC							
1	Left lateral orbital gyrus	30 384	47/12	−46	26	−10	0.080
	Left lateral orbital gyrus		47/12	−40	34	−16	0.067
	Left middle frontal gyrus		6	−44	8	38	0.060
	Left inferior frontal gyrus (pars opercularis)		44	−46	20	20	0.054
2	Left (medial) superior frontal gyrus	10 512	6	−2	12	54	0.077
	Right anterior paracingulate gyrus		32	8	28	32	0.056
	Left anterior paracingulate gyrus		32	0	30	38	0.052
3	Right inferior frontal gyrus	10 224	47	40	22	−14	0.088
	Right anterior orbital gyrus		11	28	44	−16	0.039
	Right middle frontal gyrus		10	34	56	−2	0.039
	Right middle frontal gyrus		10	34	50	−14	0.039
4	Left superior parietal lobule	3968	7	−32	−56	50	0.063
	Left inferior parietal lobule		40	−42	−52	50	0.039
5	Left caudate	1800	14	−10	4	10	0.041
	Left thalamus		15	−8	−14	10	0.036
6	Right middle frontal gyrus	1760	9	46	38	24	0.041
7	Left hippocampus	1544	35	−22	−22	−16	0.042
8	Left middle frontal gyrus	1232	10	−36	48	10	0.041
9	Right precentral gyrus	1200	6	50	8	36	0.039
	Right inferior frontal gyrus		9	48	10	26	0.033
	Right inferior frontal gyrus		9	44	18	22	0.028
10	Left precuneus	552	22	−4	−56	6	0.035
	Left posterior cingulate gyrus		29	0	−48	14	0.029
11	Right caudate	416	24	10	8	8	0.029
	Right thalamus		25	12	−4	6	0.028
12	Right thalamus	320	26	20	−30	0	0.035
13	Bilateral superior (medial) frontal gyrus	256	9	0	44	30	0.035
mOFC							
1	Left gyrus rectus/inferior frontal pole	3376	10	−8	52	−14	0.031
	Right gyrus rectus		11	2	46	−18	0.023
2	Right amygdala	1304	30	24	−2	−18	0.022
	Right amygdala		31	32	−16	−14	0.020
3	Left superior frontal gyrus	976	9	−10	60	22	0.021
4	Left amygdala	896	33	−22	−6	−16	0.022
	Left amygdala		34	−24	−12	−14	0.020
5	Left inferior frontal gyrus (pars orbitalis)	592	47/12	−52	30	−2	0.025
6	Left superior (medial) frontal gyrus	456	6	−4	8	58	0.020
7	Right inferior frontal gyrus (pars triangularis)	400	45	56	32	8	0.023
8	Left precuneus	360	31	−2	−54	36	0.017
9	Right middle temporal gyrus	312	21	60	−8	−22	0.018
10	Left middle temporal/angular gyrus	256	39	−48	−70	28	0.019

inhibition (Garavan et al. 1999; Chikazoe 2010; Levy and Wagner 2011). However, the literature on this topic usually focuses more on portions of the inferior frontal gyrus that are superior to the lOFC seed region in the present study (although as revealed by the present MACM data, these more superior elements of the ventrolateral prefrontal cortex frequently coactivate with the lOFC). Unexpectedly, of the 4 task domains analyzed in isolation, the broadest dorsomedial coactivations with the lOFC emerged during memory tasks, perhaps reflecting involvement in the regulation or inhibitory control of memory processes (Anderson et al. 2004).

Coactivation with Temporal Regions

The extent to which the OFC coactivates with medial temporal regions was notable. Both the mOFC and lOFC showed coactivations in the amygdala, which is consistent with a long tradition of anatomical data linking both the mOFC and lOFC to the amygdala (Carmichael and Price 1995a; Ghashghaei et al. 2007). Coactivations between the OFC and amygdala may occur both due to direct projections between the 2 regions and due to frequent common inputs, which allow both regions to process similar types of information (Zald and Kim 1996a). In animal tracing studies, some connections with the amygdala appear more robust in the mOFC than the lOFC (Carmichael

and Price 1995a; Ghashghaei et al. 2007). Partially consistent with this, in the contrast analysis between the mOFC and lOFC, the mOFC showed greater connectivity with the right amygdala. However, this pattern was not replicated in the left hemisphere, making it difficult to draw firm conclusions regarding preferential functional connections with the mOFC.

Significant coactivations were also seen in the hippocampus. Although the OFC is not typically a primary focus of memory research, the OFC possesses well-documented structural connections with the medial temporal lobe memory system: The subiculum/CA1 region of the hippocampus projects to the mOFC, while the entorhinal cortex has connections with both medial and lateral (area 12o) regions (Barbas 1993; Barbas and Blatt 1995; Carmichael and Price 1995a). Neuroimaging data have generally emphasized the ventrolateral prefrontal cortex as important for episodic memory retrieval (Petrides 2002; Badre and Wagner 2007), but the contribution of the OFC proper to memory has received less attention. However, OFC activations have been reported in memory studies (Elliot and Dolan 1999; Petrides 2007), lesions of the mOFC in monkeys impairs learning on classic memory tasks (Meunier et al. 1997), and lesions of the OFC in humans can produce deficits in autobiographical episodic memory (Brand and Markowitsch 2006). The MACM analysis of memory tasks revealed significant coactivation of the left

Table 10
Behavioral domain analysis: Faces

Cluster#	Region	Cluster volume (mm³)	BA	X	Y	Z	ALE
lOFC							
1	Left lateral orbital gyrus	3272	47/12	−46	26	−12	0.038
	Left posterior orbital gyrus		13	−32	16	−24	0.019
2	Right lateral orbital gyrus	2752	47/12	36	36	−14	0.033
	Right inferior frontal gyrus (pars orbitalis)		47/12	50	36	−6	0.017
3	Right middle frontal gyrus	960	46	52	30	20	0.025
4	Right fusiform gyrus	952	37	42	−54	−20	0.023
5	Left amygdala	720	28	−16	−6	−14	0.023
6	Right globus pallidus	328		26	−6	−8	0.017
mOFC							
1	Left gyrus rectus	2720	11m	−6	38	−20	0.031
	Left gyrus rectus		10	−6	52	−14	0.012
2	Left medial orbital gyrus	992	13	−16	26	−14	0.014
	Left subgenual cingulate cortex		25/32pl	−6	20	−14	0.013
3	Left hippocampus	976		−20	−12	−24	0.021
4	Right medial orbital gyrus/subgenual cingulate cortex	968	13/32pl	10	26	−14	0.019
5	Right globus pallidus	336		16	−2	−4	0.013

Table 11
Behavioral domain analysis: Semantic

Cluster#	Region	Cluster volume (mm³)	BA	X	Y	Z	ALE
lOFC							
1	Left inferior frontal gyrus/lateral orbital gyrus	21 624	47/12	−46	26	−10	0.074
	Left inferior frontal gyrus (pars opercularis/middle frontal gyrus)		9/44	−50	18	24	0.073
	Left inferior frontal gyrus/lateral orbital gyrus		47/12	−42	40	−14	0.054
	Left inferior frontal gyrus (pars triangularis)		45	−50	26	12	0.038
2	Right lateral orbital gyrus	2416	47/12	36	30	−12	0.027
	Right posterior/lateral orbital gyrus		47/12	40	16	−20	0.025
3	Left middle temporal gyrus	2000	22	−54	−38	−2	0.046
	Left middle temporal gyrus		21	−56	−30	−10	0.019
4	Bilateral superior frontal gyrus	2000	6	0	20	44	0.034
	Right paracingulate gyrus		32	8	28	34	0.022
5	Left fusiform gyrus	1680	37	−44	−52	−18	0.027
6	Right cerebellum	1192		14	−84	−30	0.037
	Right cerebellum			12	−80	−18	0.02
7	Left superior frontal gyrus	880	9	−6	56	24	0.029
8	Left angular gyrus	656	39	−40	−58	30	0.031
9	Right cuneus	376	17	12	−92	12	0.023
10	Left middle frontal gyrus	328	6	−34	12	50	0.022
11	Left hippocampus	312		−22	−12	−20	0.022
mOFC							
1	Left posterior cingulate gyrus	1760	31	0	−52	28	0.027
	Left posterior cingulate		23	−8	−56	20	0.018
	Right posterior cingulate		29/30	6	−46	18	0.016
2	Left angular gyrus	1496	39	−48	−66	30	0.02
	Left superior occipital gyrus		19	−40	−76	34	0.017
3	Left gyrus rectus	1280	10	−6	30	−18	0.027
4	Left posterior cingulate gyrus	1120	31	2	−34	38	0.023
	Left posterior cingulate gyrus		31	2	−22	40	0.014
5	Left superior frontal gyrus	632	8	−16	38	46	0.017
6	Left angular gyrus	480	39	−40	−68	42	0.013
7	Left gyrus rectus	392	11m	−4	42	−24	0.017
8	Left inferior temporal gyrus	320	37	−46	−48	−20	0.015
9	Left middle temporal gyrus	280	37	−62	−52	−8	0.013

hippocampus with the lOFC seed. By contrast, the mOFC showed coactivation with the amygdala bilaterally, and the right anterior hippocampus during memory tasks. Brand and Markowitsch (2006) suggest that the OFC's main role in episodic, particularly autobiographic, memory reflects a mediation between specific memories, memory-related emotions, and self-awareness, while Petrides (2007) has emphasized the possible importance of the OFC's processing of expectations and novelty as an influence on memory processes. Future models should attend to the potential differences in the contributions of mOFC versus lOFC regions to these processes.

A few additional discrete areas of the temporal cortex showed significant functional connectivity with the OFC. Both the mOFC and lOFC showed coactivations in focal areas of the left superior and middle temporal gyrus. Distinct mOFC and lOFC regions have been demonstrated to possess reciprocal connections to the auditory belt and parabelt regions on the superior temporal gyrus (Saleem et al. 2008), and it has been suggested that such projections could form a part of a circuit for processing affective vocalizations (Barbas 2000).

Posterior portions of the inferior temporal cortex (which are associated with the ventral visual stream) selectively coactivated with the lOFC. Neuroanatomical studies of visual afferents into the OFC support the disproportionate input of visual information into the lOFC relative to the mOFC (Barbas 1988; Carmichael and Price 1995b; Saleem et al. 2008). Inferior temporal projections may be particularly important for face processing in the OFC. lOFC, but not mOFC, activations emerge in many studies of emotional face processing (Dougherty et al. 2006; Tsao et al. 2008). Consistent with this observation, the fusiform gyrus was selectively coactivated with the lOFC, and not the mOFC, in tasks involving face processing.

Default Mode Network and Autonomic Processing
Studies of functional connectivity that rely on resting-state or intrinsic functional connectivity have repeatedly identified a

default mode network that is more active during rest than during many cognitive tasks (Raichle et al. 2001; Fox and Raichle 2007; Laird, Eickhoff, Kurth et al. 2009). This default mode is centered on ventromedial prefrontal regions (including medial orbital areas) and the posterior cingulate/retrosplenial region. The pattern of task-related functional connectivity observed in the present study recapitulates the findings from resting-state data in that mOFC showed significant coactivation with the posterior cingulate/retrosplenial region. This finding also converges with data from Greicius et al. (2003) that strong temporal covariation emerges in the ventromedial prefrontal cortex and posterior cingulate/retrosplenial cortex even during perceptual or cognitive tasks. Thus, despite very different methods of establishing functional connectivity, the same core features of a default mode network arise. A recent MACM analysis focused on the ventral anterior cingulate rather than the mOFC, reached a similar conclusion (Laird et al. 2009), reflecting the close proximity and strong
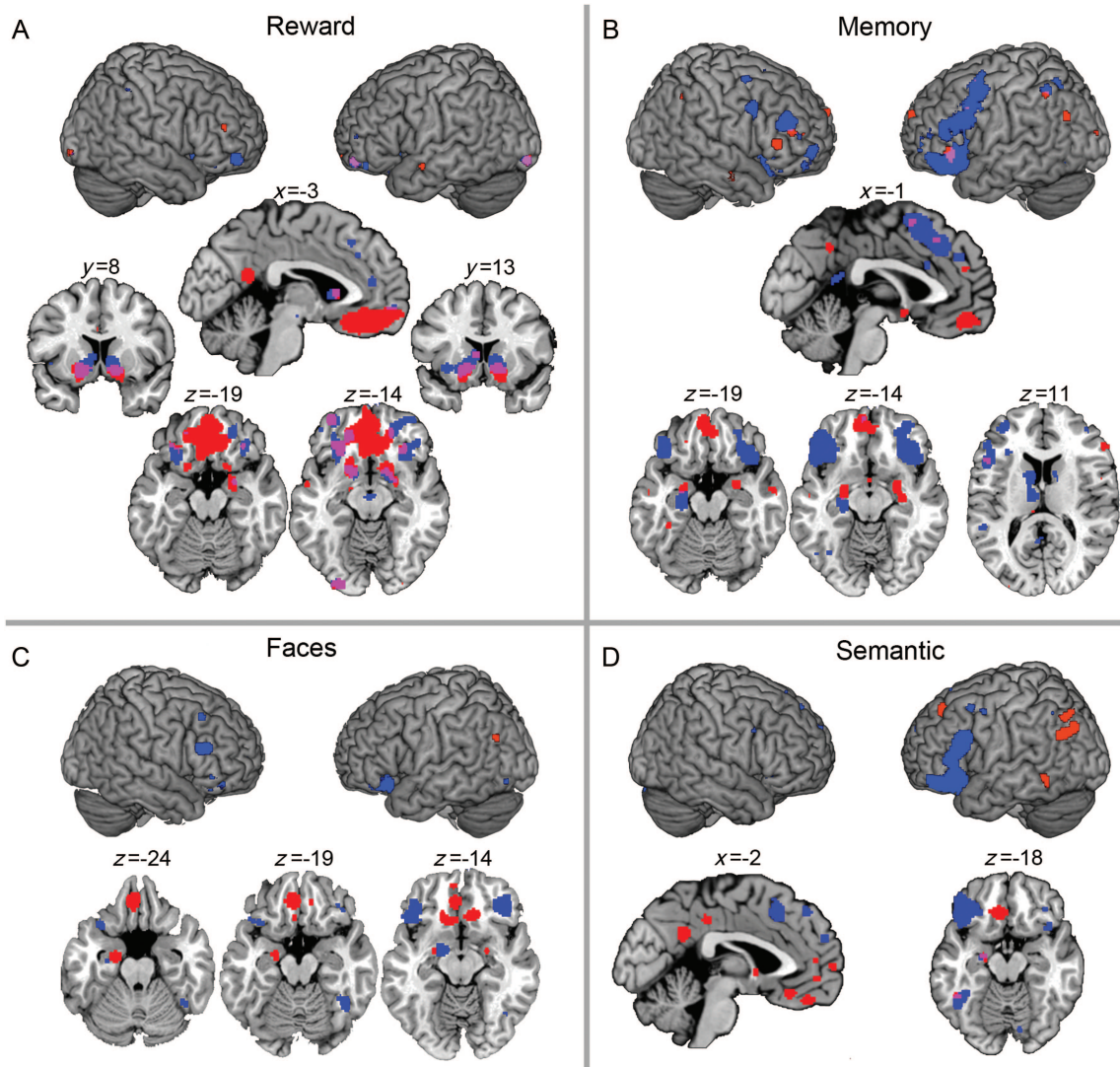
Figure 5. Significant coactivations in analyses restricted to specific functional domains. In all cases, red shows areas coactivated with the mOFC seed region, blue with the lOFC seed region, and purple with both.

functional connectivity of the medial orbital and gyrus rectus region with the ventral anterior cingulate. As observed in studies examining deactivations during tasks (Shulman et al. 1997; Laird, Eickhoff, Li et al. 2009), and resting-state analyses (Greicius et al. 2003), the lOFC is not a component of this network, a finding further supported by anatomical tracing studies demonstrating significant connections between the posterior cingulate/retrosplenial region and mOFC, but not lOFC (Saleem et al. 2008).

Ventromedial prefrontal areas have been broadly implicated in autonomic functions (Kaada and Magoun 1960), and thus, it is not surprising that a number of the regions showing coactivation with the mOFC seed are involved in autonomic functions. This was particularly notable for the posterior sector of the mOFC, which showed significant covariation with the hypothalamus, and neighboring basal forebrain and ventral striatal regions. The posterior mOFC seed region also showed coactivations limited to anterior parts of the insula that are associated with interoception and gustation, particularly in the right hemisphere (Kurth et al. 2010). Interestingly, the lOFC seed showed coactivations that included both

interoceptive and gustatory as well as more cognitive portions of the insula that activate during tasks involving working memory, memory, speech, and attention (Kurth et al. 2010).

Parietal Connectivity to the OFC

The mOFC and lOFC both showed associations with the parietal lobe, with the anterior lOFC demonstrating coactivations around the intraparietal suclus, and the mOFC showing connectivity with the angular gyrus. These findings parallel results reported by Kahnt et al. (2012) in their analysis of resting-state functional connectivity. The observed functional connectivity of the intraparietal sulcal region converges with anatomical tracing studies in Macaques, which indicate a selective projection from area 7 in the posterior parietal cortex to anterior-lateral segments of the OFC (Selemon and Goldman-Rakic 1988; Cavada and Goldman-Rakic 1989). It may be speculated that these projections provide spatial information to the OFC. While the OFC is predominantly connected to the ventral visual object processing pathway (Barbas 1988; Zald and Kim 1996a), a dorsal stream

projection could allow the anterior lOFC to integrate spatial representations or goals when they are associated with rewards or punishments as has been suggested in the rodent OFC (Feierstein et al. 2006; Roesch et al. 2006). The intraparietal sulcal region in humans has also been observed to activate during certain memory tasks (Yarkoni et al. 2011), which is notable given the emergence of coactivations of the intraparietal sulcus in the memory domain analysis of the lOFC.

The more inferior parietal (angular gyrus) connectivity with the mOFC may reflect the fact that both the mOFC and the inferior partietal cortex are associated with the default mode network (Raichle et al. 2001). There were also hints of this coactivation arising during semantic tasks. However, care must be taken in interpreting this result as the number of studies with mOFC activations in semantic processing tasks is small, and thus the analysis of coactivation for this domain must be treated with caution.

Anterior versus Posterior Distinctions

Patterns of structural connectivity have been argued to be highly influenced by the level of granularity in a given region, with dysgranular regions projecting preferentially to areas that possess similarly poorly defined cytoarchitectural features, and more granular areas preferentially projecting to more cytoarchitecturally defined areas (Barbas and Rempel-Clower 1997). Given, the dramatic increase in granularity as one moves from the posterior to anterior sectors of the OFC (Barbas and Pandya 1989; Morecraft et al. 1992), we expected significant differences to emerge in coactivations between anterior and posterior regions of the OFC. Within areas adjacent to the seed regions, this expectation was confirmed, but for more distal coactivations only a few areas showed significant differences. Indeed, in a few cases, specific a priori predictions regarding anterior–posterior differences were not born out. For instance, based on the density of connections in tracing studies in nonhuman primates (Ghashghaei et al. 2007), we expected to see significantly stronger coactivation in the amygdala for posterior than anterior OFC regions. Yet, in both the mOFC and lOFC, both the anterior and posterior sectors showed similar levels of functional connectivity. Although there are projections from the amygdala that target more anterior OFC regions, such as the anterior gyrus rectus (Carmichael and Price 1995a), we still would not have predicted such a broad pattern of coactivation based on the density of connections in more anterior OFC regions in animal studies. Assuming that the density of the projections is indeed similar to that reported by Ghashghaei et al. (2007) for monkeys, the present data may suggest a degree of coordination between anterior OFC regions and amygdala that exceeds its degree of direct anatomical connectivity. This could arise either due to common inputs or a strong indirect connection through the posterior OFC regions that are more densely structurally linked to the amygdala. For instance, more posterior mOFC areas may project forward to more anterior OFC regions providing a posterior to anterior flow of information consistent with network models of the OFC that emphasize sequential processes in the OFC with more posterior areas receiving limbic and sensory inputs that are sequentially processed in more anterior regions (Gottfried and Zald 2005; Ghashghaei et al. 2007).

Methodological Considerations

In evaluating the current findings, it is useful to note a few features of the MACM technique that may influence the observed results. First, the types of areas identified in these analyses are dependent upon the frequency of different types of functional neuroimaging studies in the BrainMap database. If certain types of cognitive, behavioral, or perceptual tasks are more frequently performed in the neuroimaging literature, they will be better represented in the database and will impact both which studies are identified as having activations in the seed region and which other brain regions have a chance of being coactivated. A similar issue arises in terms of the type of contrasts used. Some of the domains (e.g., sensory processing) are more likely to use simple contrasts with a baseline resting or fixation condition, while other higher-level domains (e.g., semantic processing) use active task contrasts. This could create a situation whereby a methodological confound influences the degree to which certain functional domains produce activations in the seed region, and the extent to which those activations are accompanied by coactivations in other regions.

Because all brain regions are not equally easy to image with fMRI, some areas may be under-represented in terms of observed activations. Such an issue is relevant in considering the mOFC as signal quality in this region (particularly the posterior mOFC) can suffer from drop out due to inhomogeneity in some fMRI studies. While such issues may have reduced the identification of studies with activations in the mOFC, there clearly were enough activations in the region to provide the ability to perform an ALE and to observe numerous statistically significant coactivations with the mOFC.

Another methodological consideration relates to ROI seed definitions. The divisions in this study were drawn purely on topographic grounds. Arguably, a more fine-grained distinction could be made with ROIs based on cytoarchitectural features. Such an approach might also allow the region to be parcellated in a manner equivalent to Carmichael and Prices's (1996) medial and orbital networks. Unfortunately, the precise boundaries of cytoarchitectural subregions in the human OFC remain difficult to define, and published boundaries are often based on single subjects making their implementation at the group level problematic (Ongür et al. 2003; Petrides and Mackey 2006). We also note that reduction to the level of cytoarchiatectural subregions would limit the statistical power of the MACM technique, as the number of observations within each small subregion would be substantially less than arises with these larger subregions. An alternative approach for future studies could utilize a metric of similarity in MACM results for different seed regions to empirically determine the ideal parcellation based on functional connectivity (Eickhoff et al. 2011). For instance, such a metric could be applied to determine the ideal dividing line between the mOFC and lOFC boundary, or whether there is enough heterogeneity to warrant the further division of an area into subregions (such as the central and extreme lateral seed regions presented in the Supplementary Analysis).

An advantage of the MACM technique relative to other techniques for examining functional connectivity is that it allows for the examination of task-related patterns of functional connectivity at different levels of task specificity or generalizability. The primary analysis, which utilized all available studies,

provides a level of generalizability that is unobtainable from individual studies that utilize a single task and a small number of subjects. By contrast, the task domain analyses revealed several context-specific aspects of OFC functional connectivity. Further elucidating the specific dynamic patterns of functional connectivity between the OFC and other regions, and the causal direction of this functional connectivity, will prove essential for understanding this region's contribution to cognition, behavior, and psychopathology.

Supplementary Material

Supplementary material can be found at: http://www.cercor.oxfordjournals.org/.

Notes

Conflict of Interest: None declared.

References

Anderson MC, Ochsner KN, Kuhl B, Cooper J, Robertson E, Gabrieli SW, Glover GH, Gabrieli JD. 2004. Neural systems underlying the suppression of unwanted memories. Science. 303:232–235.

Badre D, Wagner AD. 2007. Left ventrolateral prefrontal cortex and the cognitive control of memory. Neuropsychologia. 45:2883–2901.

Barbas H. 1988. Anatomic organization of basoventral and mediodorsal visual recipient prefrontal regions in the rhesus monkey. J Comp Neurol. 276:313–342.

Barbas H. 2000. Connections underlying the synthesis of cognition, memory, and emotion in primate prefrontal cortices. Brain Res Bull. 52:319–330.

Barbas H. 1993. Organization of cortical afferent input to orbitofrontal areas in the rhesus monkey. Neuroscience. 56:841–864.

Barbas H. 2007. Specialized elements of orbitofrontal cortex in primates. Ann N Y Acad Sci. 1121:10–32.

Barbas H, Blatt GJ. 1995. Topographically specific hippocampal projections target functionally distinct prefrontal areas in the rhesus monkey. Hippocampus. 5:511–533.

Barbas H, Pandya DN. 1989. Architecture and intrinsic connections of the prefrontal cortex in the rhesus monkey. J Comp Neurol. 286:353–375.

Barbas H, Rempel-Clower N. 1997. Cortical structure predicts the pattern of corticocortical connections. Cereb Cortex. 7:635–646.

Bates JF, Goldman-Rakic PS. 1993. Prefrontal connections of medial motor areas in the rhesus monkey. J Comp Neurol. 336:211–228.

Bokde AL, Tagamets MA, Friedman RB, Horwitz B. 2001. Functional interactions of the inferior frontal cortex during the processing of words and word-like stimuli. Neuron. 30:609–617.

Bookheimer SY, Zeffiro TA, Blaxton T, Gaillard W, Theodore W. 1995. Regional cerebral blood flow during object naming and word reading. Hum Brain Mapp. 3:93–106.

Brand M, Markowitsch HJ. 2006. Memory processes and the orbitofrontal cortex. In: Zald DH, Rauch SL, editors. The orbitofrontal cortex. Oxford, UK: Oxford University Press. p. 285–306.

Carmichael ST, Price JL. 1994. Architectonic subdivision of the orbital and medial prefrontal cortex in the macaque monkey. J Comp Neurol. 346:366–402.

Carmichael ST, Price JL. 1996. Connectional networks within the orbital and medial prefrontal cortex of macaque monkeys. J Comp Neurol. 371:179–207.

Carmichael ST, Price JL. 1995a. Limbic connections of the orbital and medial prefrontal cortex in macaque monkeys. J Comp Neurol. 363:615–641.

Carmichael ST, Price JL. 1995b. Sensory and premotor connections of the orbital and medial prefrontal cortex of macaque monkeys. J Comp Neurol. 363:642–664.

Cavada C, Compañy T, Tejedor J, Cruz-Rizzolo RJ, Reinoso-Suárez F. 2000. The anatomical connections of the macaque monkey orbitofrontal cortex. A review. Cereb Cortex. 10:220–242.

Cavada C, Goldman-Rakic PS. 1989. Posterior parietal cortex in rhesus monkey: II. Evidence for segregated corticocortical networks linking sensory and limbic areas with the frontal lobe. J Comp Neurol. 287:422–445.

Chiavaras MM, LeGoualher G, Evans A, Petrides M. 2001. Three-dimensional probabilistic atlas of the human orbitofrontal sulci in standardized stereotaxic space. Neuroimage. 13:479–496.

Chikazoe J. 2010. Localizing performance of go/no-go tasks to prefrontal cortical subregions. Curr Opin Psychiatry. 23:267–272.

Croxson PL, Johansen-Berg H, Behrens TE, Robson MD, Pinsk MA, Gross CG, Richter W, Richter MC, Kastner S, Rushworth MF. 2005. Quantitative investigation of connections of the prefrontal cortex in the human and macaque using probabilistic diffusion tractography. J Neurosci. 25:8854–8866.

Dehaene S, Dupoux E, Mehler J, Cohen L, Paulesu E, Perani D, van de Moortele PF, Lehericy S, Le Bihan D. 1997. Anatomical variability in the cortical representation of first and second language. Neuroreport. 8:3809–3815.

Dougherty D, Shin L, Rauch SL. 2006. Orbitofrontal cortex activation during functional neuroimaging studies of emotion induction in humans. In: Zald DH, Rauch SL, editors. The orbitofrontal cortex. Oxford, UK: Oxford University Press. p. 377–392.

Eickhoff SB, Bzdok D, Laird AR, Kurth F, Fox PT. 2012. Activation likelihood estimation meta-analysis revisited. Neuroimage. 59:2349–2361.

Eickhoff SB, Bzdok D, Laird AR, Roski C, Caspers S, Zilles K, Fox PT. 2011. Co-activation patterns distinguish cortical modules, their connectivity and functional differentiation. Neuroimage. 57:938–949.

Eickhoff SB, Grefkes C. 2011. Approaches for the integrated analysis of structure, function and connectivity of the human brain. Clin EEG Neurosci. 42:107–121.

Eickhoff SB, Jbabdi S, Caspers S, Laird AR, Fox PT, Zilles K, Behrens TE. 2010. Anatomical and functional connectivity of cytoarchitectonic areas within the human parietal operculum. J Neurosci. 30:6409–6421.

Eickhoff SB, Laird AR, Grefkes C, Wang LE, Zilles K, Fox PT. 2009. Coordinate-based activation likelihood estimation meta-analysis of neuroimaging data: a random-effects approach based on empirical estimates of spatial uncertainty. Hum Brain Mapp. 30:2907–2926.

Elliott R, Dolan RJ. 1999. Differential neural responses during performance of matching and nonmatching to sample tasks at two delay intervals. J Neurosci. 19:5066–5073.

Feierstein CE, Quirk MC, Uchida N, Sosulski DL, Mainen ZF. 2006. Representation of spatial goals in rat orbitofrontal cortex. Neuron. 51:495–507.

Fox MD, Raichle ME. 2007. Spontaneous fluctuations in brain activity observed with functional magnetic resonance imaging. Nat Rev Neurosci. 8:700–711.

Garavan H, Ross TJ, Stein EA. 1999. Right hemispheric dominance of inhibitory control: an event-related functional MRI study. Proc Natl Acad Sci USA. 96:8301–8306.

Ghashghaei HT, Hilgetag CC, Barbas H. 2007. Sequence of information processing for emotions based on the anatomic dialogue between prefrontal cortex and amygdala. Neuroimage. 34:905–923.

Gottfried JA, Zald DH. 2005. On the scent of human olfactory orbitofrontal cortex: meta-analysis and comparison to non-human primates. Brain Res Brain Res Rev. 50:287–304.

Greicius MD, Krasnow B, Reiss AL, Menon V. 2003. Functional connectivity in the resting brain: a network analysis of the default mode hypothesis. Proc Natl Acad Sci USA. 100:253–258.

Hof PR, Mufson EJ, Morrison JH. 1995. Human orbitofrontal cortex: cytoarchitecture and quantitative immunohistochemical parcellation. J Comp Neurol. 359:48–68.

Holmes CJ, Hoge R, Collins L, Woods R, Toga AW, Evans AC. 1998. Enhancement of MR images using registration for signal averaging. J Comput Assist Tomogr. 22:324–333.

Ioannides AA. 2007. Dynamic functional connectivity. Curr Opin Neurobiol. 17:161–170.

Kaada BR, Magoun HW. 1960. Cingulate, posterior orbital, anterior insular, and temporal pole cortex. In: Field F, Magoun HW, Hall VE, editors. Handbook of physiology. Washington (DC): American Physiological Society. p. 1345–1372.

Kahnt T, Chang LJ, Park SQ, Heinzle J, Haynes JD. 2012. Connectivity-based parcellation of the human orbitofrontal cortex. J Neurosci. 32:6240–6250.

Kringelbach ML, Rolls ET. 2004. The functional neuroanatomy of the human orbitofrontal cortex: evidence from neuroimaging and neuropsychology. Prog Neurobiol. 72:341–372.

Kurth F, Zilles K, Fox PT, Laird AR, Eickhoff SB. 2010. A link between the systems: functional differentiation and integration within the human insula revealed by meta-analysis. Brain Struct Funct. 214:519–534.

Laird AR, Eickhoff SB, Fox PM, Uecker AM, Ray KL, Saenz JJ Jr, McKay DR, Bzdok D, Laird RW, Robinson JL et al. 2011. The BrainMap strategy for standardization, sharing, and meta-analysis of neuroimaging data. BMC Res Notes. 9:349.

Laird AR, Eickhoff SB, Kurth F, Fox PM, Uecker AM, Turner JA, Robinson JL, Lancaster JL, Fox PT. 2009. ALE meta-analysis workflows via the brainmap database: progress towards a probabilistic functional brain atlas. Front Neuroinformatics. 3:23.

Laird AR, Eickhoff SB, Li K, Robin DA, Glahn DC, Fox PT. 2009. Investigating the functional heterogeneity of the default mode network using coordinate-based meta-analytic modeling. J Neurosci. 29:14496–14505.

Laird AR, Robinson JL, McMillan KM, Tordesillas-Gutierrez D, Moran ST, Gonzales SM, Ray KL, Franklin C, Glahn DC, Fox PT, Lancaster JL. 2010. Comparison of the disparity between Talairach and MNI coordinates in functional neuroimaging data: validation of the Lancaster transform. Neuroimage. 51:677–683.

Lancaster JL, Tordesillas-Gutierrez D, Martinez M, Salinas F, Evans A, Zilles K, Mazziotta JC, Fox PT. 2007. Bias between MNI and Talairach coordinates analyzed using the icbm-152 brain template. Hum Brain Mapp. 2811:1194–1205.

Levy BJ, Wagner AD. 2011. Cognitive control and right ventrolateral prefrontal cortex: reflexive reorienting, motor inhibition, and action updating. Ann N Y Acad Sci. 1224:40–62.

Luke KK, Liu HL, Wai YY, Wan YL, Tan LH. 2002. Functional anatomy of syntactic and semantic processing in language comprehension. Hum Brain Mapp. 16:133–145.

Mai JK, Assheuer, Paxinos G. 1997. Atlas of the Human Brain. San Diego, CA: Academic Press.

Malykhin N, Vahidy S, Michielse S, Coupland N, Camicioli R, Seres P, Carter R. 2011. Structural organization of the prefrontal white matter pathways in the adult and aging brain measured by diffusion tensor imaging. Brain Struct Funct. 216:417–31.

Meunier M, Bachevalier J, Mishkin M. 1997. Effects of orbital frontal and anterior cingulate lesions on object and spatial memory in rhesus monkeys. Neuropsychologia. 35:999–1015.

Morecraft RJ, Geula C, Mesulam MM. 1992. Cytoarchitecture and neural afferents of orbitofrontal cortex in the brain of the monkey. J Comp Neurol. 323:341–358.

O'Doherty J, Dolan R. 2006. The role of human orbitofrontal cortex in reward prediction and behavioral choice: insights from neuroimaging. In: Zald DH, Rauch SL, editors. The orbitofrontal cortex. Oxford, UK: Oxford University Press. p. 265–284.

Ongür D, Ferry AT, Price JL. 2003. Architectonic subdivision of the human orbital and medial prefrontal cortex. J Comp Neurol. 460:425–449.

Papathanassiou D, Etard O, Mellet E, Zago L, Mazoyer B, Tzourio-Mazoyer N. 2000. A common language network for comprehension and production: a contribution to the definition of language epicenters with PET. Neuroimage. 11:347–357.

Petrides M. 2002. The mid-ventrolateral prefrontal cortex and active mnemonic retrieval. Neurobiol Learn Mem. 78:528–538.

Petrides M. 2007. The orbitofrontal cortex: novelty, deviation from expectation, and memory. Ann N Y Acad Sci. 1121:33–53.

Petrides M, Mackey S. 2006. The orbitofrontal cortex: sulcal and gyral morphology and architecture. In: Zald DH, Rauch SL, editors. The orbitofrontal cortex. Oxford, UK: Oxford University Press. p. 19–38.

Petrides M, Pandya DN. 2002. Comparative cytoarchitectonic analysis of the human and the macaque ventrolateral prefrontal cortex and corticocortical connection patterns in the monkey. Eur J Neurosci. 16:291–310.

Price JL. 2007. Definition of the orbital cortex in relation to specific connections with limbic and visceral structures and other cortical regions. Ann N Y Acad Sci. 1121:54–71.

Raichle ME, MacLeod AM, Snyder AZ, Powers WJ, Gusnard DA, Shulman GL. 2001. A default mode of brain function. Proc Natl Acad Sci USA. 98:676–682.

Ridderinkhof KR, Ullsperger M, Crone EA, Nieuwenhuis S. 2004. The role of the medial frontal cortex in cognitive control. Science. 306:443.

Robinson J, Laird A, Glahn D, Lovallo W, Fox P. 2010. Metaanalytic connectivity modeling: delineating the functional connectivity of the human amygdala. Hum Brain Mapp. 31:173–184.

Roesch MR, Taylor AR, Schoenbaum G. 2006. Encoding of time-discounted rewards in orbitofrontal cortex is independent of value representation. Neuron. 51:509–520.

Saleem KS, Kondo H, Price JL. 2008. Complementary circuits connecting the orbital and medial prefrontal networks with the temporal, insular, and opercular cortex in the macaque monkey. J Comp Neurol. 506:659–693.

Selemon LD, Goldman-Rakic PS. 1988. Common cortical and subcortical targets of the dorsolateral prefrontal and posterior parietal cortices in the rhesus monkey: evidence for a distributed neural network subserving spatially guided behavior. J Neurosci. 8:4049–4068.

Shulman GI, Fiez J, Corbetta M, Buckner RL, Miezin FM, Raichle M, Petersen SE. 1997. Common blood flow changes across visual tasks: II. Decreases in cerebral cortex. J Cogn Neurosci. 9:648–663.

Small DM, Zatorre RJ, Dagher A, Evans AC, Jones-Gotman M. 2001. Changes in brain activity related to eating chocolate–from pleasure to aversion. Brain. 124:1720–1733.

Tsao DY, Schweers N, Moeller S, Freiwald WA. 2008. Patches of face-selective cortex in the macaque frontal lobe. Nat Neurosci. 11:877–879.

Turkeltaub PE, Eden GF, Jones KM, Zeffiro TA. 2002. Meta-analysis of the functional neuroanatomy of single-word reading: method and validation. Neuroimage. 16:765–780.

Turkeltaub PE, Eickhoff SB, Laird AR, Fox M, Wiener M, Fox P. 2012. Minimizing within-experiment and within-group effects in activation likelihood estimation meta-analyses. Hum Brain Mapp. 33:1–13.

Uylings HBM, Sanz-Arigita EJ, de Vos K, Pool CW, Evers P, Rajkowska G. 2010. 3-d cytoarchitectonic parcellation of human orbitofrontal cortex correlation with postmortem MRI. Psychiatry Res. 183:1–20.

Vanlancker-Sidtis D, McIntosh AR, Grafton S. 2003. PET activation studies comparing two speech tasks widely used in surgical mapping. Brain Lang. 85:245–261.

Walker AE. 1940. A cytoarchitectural study of the prefrontal area of the macaque monkey. J Comp Neurol. 73:59–86.

Yarkoni T, Poldrack RA, Nichols TE, Van Essen DC, Wager TD. 2011. Large-scale automated synthesis of human functional neuroimaging data. Nat Methods. 8:665–670.

Zald DH, Kim SW. 1996a. Anatomy and function of the orbital frontal cortex. I: anatomy, neurocircuitry; and obsessive-compulsive disorder. J Neuropsychiatry Clin Neurosci. 8:125–138.

Zald DH, Kim SW. 1996b. Anatomy and function of the orbital frontal cortex. II: function and relevance to obsessive-compulsive disorder. J Neuropsychiatry Clin Neurosci. 8:249–261.

Zald DH, Rauch SL, editors. 2006. The orbitofrontal cortex Oxford, UK: Oxford University Press.